Warming summer temperatures are rapidly restructuring North American bumble bee communities

Jeremy Hemberger[1] *, Neal Williams[1]

[1] Department of Entomology and Nematology, University of California Davis. One Shields Ave, Davis, CA 95616 USA

* Corresponding author address: Department of Entomology, University of Wisconsin-Madison. 1630 Linden Dr, Madison, WI 53706

Phone: (608) 622-2698

Email address: j.a.hemberg@gmail.com

Running title: Warming restructures bumble bee communities

Keywords: Climate change, bumble bee, community temperature index, ecoinformatics, community composition

Abstract

A rapidly warming climate is a primary force driving changes in biodiversity worldwide. The impact of warming temperatures on insect communities is of particular interest given their importance for ecosystem function and service provision and the uncertainty around whether insect communities can keep pace with the rate of increasing temperatures. We use a long-term dataset on bumble bee species occurrence along with summer maximum temperature trends across North America to characterize community-level responses to recent climate warming. We examined responses using the community temperature index (CTI) – a measure of the balance of cool- and warm-adapted species within local communities. Starting in 2010, bumble bee average CTI across North America has rapidly increased after a period of slight increase from 1989 to the late 2000s. This increase is strongly associated with recent increases in maximum summer temperatures. The increase in CTI is spatially extensive, but the areas exhibiting the largest increase include mid to high latitudes as well as low and high elevations - areas relatively shielded from other intensive global changes (e.g., land-use). On average, bumble bee CTI has increased 0.99°C from 1989 to 2018, a change of similar magnitude to the increase in maximum summer temperatures. This shift has been driven by the rapid loss of cold-adapted species and an increase in warm-adapted species within bumble bee communities across North American ecosystems. Despite evidence that the spatial velocity of community change is keeping pace with temperatures, this is a direct result of the decline of cool-adapted species. Our results provide strong evidence of the pervasive impacts posed to insect communities by temperature increases in the last 30 years.

Introduction

Climate change is driving profound changes in animal occurrence and community composition worldwide. Long-term increases in average temperature as well as increases in acute, extreme weather events (e.g., heat waves) have been linked to both positive (Kammerer et al., 2021; Crossley et al., 2021) and negative outcomes for biodiversity (Kammerer et al., 2021; Oliver et al., 2016; Outhwaite et al., 2022; Sirois-Delisle & Kerr, 2018). Regardless of the direction of such outcomes, a rapidly changing climate has the potential to fundamentally alter biological processes, including ecosystem services that maintain biodiversity and support global agricultural production (Johnson et al., 2023; Settele et al., 2016).

Insect responses to climate change are of specific interest given the growing documentation of declines in a variety of taxa and regions (Halsch et al., 2021; Raven & Wagner, 2021). Although several anthropogenic drivers of global change are at play (Goulson et al., 2015; Hemberger et al., 2021), a changing climate is particularly menacing given the number of potential direct and indirect impacts it has on insects and its capacity to be a force-multiplier, interacting with other factors to exacerbate changes in insect populations (Hoover et al., 2012; Forrest et al., 2018; Kenna et al., 2023). Like many global change drivers, rapidly increasing temperatures may favor some species while leading to local extirpations of others. Though temperatures above the critical limits of species (e.g., CT_{max}; Oyen et al., 2018) are unlikely, the extent to which climate warming has contributed to local shifts in insect abundance and community structure remains mostly unknown. This knowledge gap places our understanding of a host of ecological processes and services in limbo.

Even among the most studied insect taxa there is debate about the extent, severity, and direction of effects associated with climate change. Bumble bees are a prime example with some studies revealing extensive declines (Soroye et al., 2020; but see Guzman et al., 2021) and others suggesting resilience and relative stability (Guzman et al., 2021; Maebe et al., 2021) or mixed patterns of decline and increases over time (Jackson et al., 2022). Most current approaches examining the long-term influence of climate on bumble bees use occupancy models to relate changes in species occurrence to trends in climate, such as increases in temperature and changes in precipitation (Janousek et al., 2023). Although this method yields valuable insights, it can be challenging to align the framework with the incidental and imperfect occurrence data that abounds in large-scale insect databases, making model outcomes sensitive to occupancy assumptions (Guzman et al., 2021). Moreover, the occupancy approach framework does not explicitly capture any physiological mechanisms driving species responses to warming temperatures. As such, a more thorough understanding of where/when insects are most impacted by climate change requires exploring alternative analytical methods that better tie climatic changes to estimates of insect physiological temperature preferences and limits.

We characterize bumble bee community responses to recent climate warming at the continental scale by examining changes in the community temperature index (CTI), a physiologically-informed metric of community responses to climate based on the composition of cool- and warm-adapted species. This metric can be used to assess the rate of change in community composition based on historical species temperature preferences

(species temperature index, STI), as well as the spatial velocity of community changes (Devictor et al., 2008, 2012). When examined over time associated with temperature, CTI can help determine whether species are keeping pace with the velocity of temperature trends (i.e., an increase in warm-adapted species and a loss of cool-adapted species in rapidly warming areas; Fourcade et al. 2019), or whether communities are accruing "climate debts", as rising temperatures outpace species turnover (Devictor et al., 2012).

Using 50 years of records from the Bumble bees of North America database (Richardson 2023), we test for changes in bumble bee communities using CTI across North America by quantifying the association between changes in CTI with trends in maximum summer temperature. Specifically, we wanted to address the following questions: (1) is there evidence of an increase in bumble bee CTI over time? (2) are changes in CTI associated with increases in summer temperatures? (3) are CTI changes greater in areas particularly vulnerable to a changing climate (e.g., higher latitudes and elevations)? and (4) is a loss of cool-adapted or an increase in warm-adapted species driving the observed changes in CTI? We predicted a steady increase in bumble bee CTI in accordance with documented increases in average maximum summer temperatures over the past century and that changes would be more dramatic at higher latitudes and elevations. We also expected that a host of common, warm-adapted species that have increased in occurrence over the past several decades would be the strongest drivers of change in CTI across the continent.

Methods

North American bumble bee occurrence and community data

We used occurrence records for 59 species of North American bumble bees from the bumble bees of North America database (BBNA; Richardson 2023). This database composes 781,280 records from 1805-2020 from a variety of sources (e.g., natural history collections, research studies, citizen science programs). To match the temporal range of available climate data, we used bumble bee records collected between 1960 and 2018. Because the database consists of an amalgam of sources, we took several steps to account for known biases (Bartomeus et al., 2019; Gotelli et al., 2021). The species and community temperature indices at large scales of our analysis are robust to imprecision in the underlying distributional data (Devictor et al., 2008); nonetheless we filtered the original dataset to include only complete records (i.e., identified to species, containing complete coordinates) and unique collection events (distinct combinations of species, date, coordinates, and observer; Figure 1A). This step helps to minimize the bias associated with unequal sampling efforts and differential data collection methods across all observers. Moreover, we conducted a range of sensitivity analyses (see below) to determine whether our results were robust given our assumptions and methodological decisions.

Is there evidence of an increase in bumble bee CTI over time?

Calculating the CTI first requires us to determine the species temperature index (STI; the historical average summertime temperature experienced over a species' approximate range; Figure 1B) for all species present within a given community. For this calculation, we used summer maximum monthly temperature as the bulk of bumble bee records are collected during this period corresponding the peak flight for most North American species. To calculate the STI, we used a subset of bee occurrence records from 1960-2000 to extract historical summertime temperatures at these locations from a global climate database. The purpose of extracting these records is to delineate the approximate range of each species. Because the range estimates for North American bumble bees are largely based on records from this dataset (Williams et al. 2014), we are confident that these data capture the range of almost all included species. Next, using the `raster` package (Hijmans, 2023), we calculated the historical average maximum summer temperatures at the specific location (i.e., raster pixel) of each occurrence record for that species from the WorldClim version 2.1 historical climate database at 30 arc-second (~1 km^2) resolution (Fick & Hijmans, 2017) by averaging the maximum monthly temperature for summer months (defined here as June-September) for a historical period of 1970 to 2000. We used this historical dataset as it is the highest resolution historical temperature raster available through WorldClim. We then used this raster to extract mean summer maximum temperature values using our bumble bee occurrence records. For each species, we then calculated the mean of the extracted values to determine the STI estimate.

Use of the CTI framework required us to assign bee occurrence records to communities to calculate CTI values for given locations/times (Devictor et al., 2008; Figure 1C). To do this, we created a hexagonal grid across North America at a broad spatial scale (50 km hexagonal grid resolution, center to side: ~ 6600 km2) to act as stand-in "community" boundaries. We chose a 50 km resolution to ensure we would capture sufficient records

within each grid cell to robustly estimate the broad spatiotemporal trend of CTI (Jackson et al., 2022). Although these species assemblages are considerably larger than the scale of an ecological community, the analysis is ultimately agnostic to this point, and it does not affect our specific questions. We refer to them as communities/CTI to maintain consistency with the existing literature. Also, because we used occurrence records from a variety of sources whose spatial locations varied over time, using fixed sampling locations to delineate communities (e.g., Prince and Zuckerberg 2014) was not possible. To determine if the resolution of our grid cells impacted our results, we also conducted our analyses using 25 and 100 km center-to-side hexagonal grid cells. Using these grids, we assigned bumble bee occurrence records to each cell to create quasi-communities, requiring each cell to contain at least 2 species for a given year to calculate CTI. We used hexagonal grid cells to minimize possible edge effects and provide a better fit across the curvature of the earth at large spatial scales (e.g., continental; Birch et al. 2007).

Using STI values, we then calculated CTI within each grid cell where at least 2 species records were present in the grid using the full set of bumble bee occurrence records from 1989-2018 (Figure 1D). We were limited to using only CTI calculations from 1989 onward as 1989 was the first year for which we could calculate a 30-year moving average summer temperature anomaly (see below). We calculated CTI using two different methods, first using occurrence records for species *i* occurring within a given community (grid cell) *j*

$$Equation\ 1\text{: }Occurrence\ CTI_j = \frac{\sum_{i=1}^{n} STI_{i,j}}{n}$$

and then using abundance weighted estimates of species within each community:

$$Equation\ 2\text{: }Abundance\ weighted\ CTI_j = \frac{\sum_{i=1}^{n} a_{i,j} \times STI_{i,j}}{\sum_{i=1}^{n} a_{i,j}}$$

where $a_{i,j}$ is the abundance of species *i* at site *j*, and *n* is the total number of species within a grid cell (Princé & Zuckerberg, 2015). In our case, the true abundance is not known, but we use the total number of individuals of species *i* within the community of bees at site *j*, the grid cell, as a proxy of abundance. These two approaches, though similar, estimate the two mechanisms of change in CTI. Using occurrence records (Equation 1) allowed us to test shifts in CTI due to changes in occurrence (i.e., immigration/extirpation), while calculating CTI using abundance weighting (Equation 2) allowed us to understand shifts in CTI as a function of changes in local relative abundance (i.e., species becoming more common/rare within a given community).

Are changes in CTI associated with increases in summer temperatures?

To determine long-term warming trends across North America, we used WorldClim gridded historical monthly weather data from 1961-2018 for our defined summer months (Fick & Hijmans, 2017). First, we averaged the maximum monthly temperature for each year. Second, we extracted the mean maximum temperature within each of the bumble bee community grid cells (Figure 1E). This procedure created a time series of the average maximum summer temperature for each year/grid cell from 1961-2018. Third, we calculated the average maximum summer temperature for a historical period from 1961-2000 for each grid cell; this is our baseline, and we refer to it as the temperature “normal”.

Last, we calculated the summer maximum temperature anomaly (defined here as the deviation from long-term normal) and averaged these using 3 moving-window scales of 3, 10, and 30 years to capture metrics of relatively short-, medium-, and long-term changes in maximum summer temperatures, respectively. To illustrate the estimated trends in maximum summertime temperatures, we calculated the change in our 3 scales of anomalies by subtracting the 1989 average anomaly (first possible year to calculate 30-year average) from the 2018 average anomaly for each grid cell. This meant that, when modeling change in CTI as a function of temperature anomalies, modeled from 1989-2018 (i.e., where all measures had maximum temperature anomaly values for all three scales (3-, 10-, and 30-year).

We used generalized additive models (GAM) to quantify trends in CTI over space and time and determine whether changes in CTI were related to short-, medium-, and long-term trends in temperature anomalies (Figure 1F). Generalized additive models provide a highly flexible computational framework to account for variable trends in spatiotemporal processes (Pedersen et al., 2019) and are especially well-suited for the analysis of potentially complex time series and can readily identify periods of significant change (Simpson, 2018).

For each measure of CTI (occurrence and abundance-weighted), we fitted a GAM to model the effects of spatial location (latitude, longitude, and elevation), long-term trend (year), short-, medium-, and long-term estimates of rising temperatures (3, 10, and 30-year summertime maximum temperature anomalies). For the remainder of this manuscript, we refer to this GAM as the global model.

$$Equation\ 3: CTI_j \sim s(lat, long) + s(year) + s(elevation) + ti(lat, long, year, elevation) + s(eco\ region, bs = \text{"re"}) + \mathrm{s}(\bar{T}_{\max 3}) + \mathrm{s}(\bar{T}_{\max 10}) + \mathrm{s}(\bar{T}_{\max 30})$$

We fit the model using the mgcv package in R (Wood, 2011). The goal of each model was to identify the spatiotemporal trend in CTI along with its statistical association with changes in summertime maximum temperatures. Because of the differences in geography, land-use, and climate across North America, we included a 2-dimensional smooth of latitude and longitude, and we allowed the estimated temporal trend in CTI to vary according to spatial location by including a tensor product interaction of latitude, longitude, elevation, and year (Pedersen et al., 2019; Equation 3). We also included a random effect smooth of ecological region (Omernik, 1987) to further account for variation in the response of CTI associated with common biophysical characteristics within ecological regions, such as commonalities in vegetation and other climate variables (e.g., precipitation). We used the Level 1 ecoregions defined and maintained by the US EPA (Omernik and Griffith. 2014). We included smooths of 3-, 10-, and 30-year summertime maximum temperature anomalies to determine whether changes in CTI were correlated with trends in warming maximum summer temperatures. Including three different anomaly scales allowed us to coarsely estimate the temporal scale of temperature change to which bumble bee communities respond most strongly to. This model was fit to CTI estimates from 1989-2018 as 1989 was the first year for which 30-year temperature anomalies could be calculated for each grid cell. We tested the model for spatial and temporal autocorrelation in the residuals. For spatial autocorrelation, we tested simulated residuals with a Moran's I test using the DHARMa package (Hartig, 2022). For temporal autocorrelation, we visually examined the

autocorrelation function using scaled, simulated residuals, finding no evidence of problematic residual correlation.

To visualize the change in CTI over time, we generated CTI predictions across the spatial and temporal extents of our dataset using the global model for each grid cell. We then determined the change in CTI from 1989-2018 by subtracting the modeled CTI estimate for 1989 from that of 2018 for each grid cell. To visualize model uncertainty, we calculated the average standard error of global model predictions for each grid cell from 1989-2018. We visualized the effect of the three moving-average temperature anomalies on CTI by plotting the partial effects (prediction of CTI as a function of temperature holding other variables are at their mean value) of each anomaly from the global model using the gratia (Simpson, 2023) package.

Are CTI changes greater in areas particularly vulnerable to a changing climate (e.g., higher latitudes and elevations)?

To determine whether CTI changes were most drastic (i.e., greater slope in fitted GAM) in areas known to be experiencing accelerated climatic changes, we examined the rate of change in the slope (i.e., derivative) of our fitted model smooth (Figure S1). To do this, we first fitted a GAM to CTI predictions with a single smooth of year to create a spatially explicit, estimated trend of CTI for each grid cell. Then, for each grid cell's fitted GAM year smooth, we extracted the first derivative with respect to time (1990-2018) using the derivatives() function from the gratia package (Simpson, 2023). For elevation and latitude, we calculated the mean derivative value for each grid cell (i.e., the average rate of change of the CTI of a grid cell from 1989-2018) and then plotted this against the mean elevation and latitude of the grid cell. We visualized the relationship with a GAM fit using the geom_smooth() function in the ggplot (Wickham et al., 2019) package. To determine whether CTI changes were consistent or have accelerated over time, we calculated the derivative values for the year smooth for each grid cell and plotted these values against the year. Like elevation, this relationship was visualized with a simple GAM fit.

Which species are driving any observed changes in CTI?

Although quantifying the trend in CTI provides evidence for whether communities are being restructured in response to a changing climate, the procedure does not identify the mechanism driving changes. For example, for areas where CTI is observed to increase, is it an increase in warm-adapted or a decrease in cool-adapted driving the change? To address this, we modeled the trend in the relative abundance of cool- and warm-adapted species to generalize the mechanism underlying the observed changes in CTI across North America. First, we assigned species as either cool- or warm-adapted within each grid cell by comparing species STI values against the average of STI values (i.e., the CTI) across all species present within the cell. STI values above the community mean were assigned "warm-adapted" while those below were assigned "cool-adapted". This approach allowed species identified as cool- or -warm adapted to change based on the location and community composition, which we felt was more realistic than assigning cool- or warm-adapted based on a range-wide assessment given that some species have extensive ranges that cover large swaths of North America. Next, we calculated the relative abundance of each species in each grid cell within 3 temporal bins (each with ~ equal numbers of

observations). For each species, we then fit a binomial GLMM with a fixed effect of the year bin and a random effect of ecological region to estimate the temporal trend in relative abundance across all grid cells where the species was present. Modeling relative abundance in this way is a useful proxy to determine approximate trends in species occurrence and abundance (Hemberger et al., 2021, Gotelli et al., 2021). Next, we extracted the model coefficient for the year bin term and combined these estimates with species occurrence records that were assigned as either cool- or warm-adapted. We then fit a subsequent GLM that predicted the estimated relative abundance trend as a function of species thermal group (cool- or warm adapted) and its interaction with the latitude of the grid cell of the observation and an error propagation term. Because this model was fit using coefficients from the species-specific relative abundance trend models, we included the error propagation term (coefficient standard error / coefficient estimate) to help account for the uncertainty in the underlying coefficient estimates. This model allowed us to determine whether the rate of change in relative abundance among the two species groups varied from South to North given known trends in increasing temperatures across latitudes.

Model validation

We performed cross validation on our global model using testing data that was filtered out of the full BBNA database. These collection events, while not "unique" (i.e., not necessarily fully independent given our strict definition), were still valid records that could be used to calculate the CTI for any given location. Upon calculating the CTI for grid cells using these records, we compared the values against predictions from the global model by using the coefficient of determination (R2), root mean square error (RMSE) and mean absolute error (MAE).

Despite the vast number of individual occurrence records within our dataset, there were many grid cells that did not contain species occurrence data for fitting the model. Given that we explicitly model CTI over space, we presented our results above using predictions within all grid cells given the strength of our global model fits. However, we also assessed the results when using model predicted values of CTI only for grid cells containing occurrence data. This approach was primarily meant to provide conservative estimates of CTI changes, particularly where in space (i.e., latitude, elevation) and time changes have been the largest.

We conducted all data wrangling, GIS operations, modeling, and visualization using R (R Core Team, 2017) using the aforementioned and following packages: tidyverse (Wickham et al., 2019), raster (Hijmans, 2023), sf (Pebesma, 2018), performance (Lüdecke et al., 2021), janitor (Firke, 2021), paletteer (Hvitfeldt, 2021), exactextractr (Daniel Baston, 2022), foreach (Microsoft & Weston, 2022), and data.table (Dowle & Srinivasan, 2023) packages.

Results

Bumble bee community temperature index has increased across a majority of North America

From 1989-2018 bumble bee CTI increased substantially across most of North America. Overall, CTI increased on average 0.99 ± 1.98 °C (mean ± SD). The magnitude of change in CTI was spatially variable, ranging from a decrease of 6.30 °C to an increase of 7.99 °C (Figure 2A). The predictions were most certain across the coterminous United States where there is a high density of bumble bee records and less certain in the most northern grid cells of our study region in the high Tundra and Queen Elizabeth Islands as well as in the tropical wet forests of Mexico (Figure 2B). The spatial trends of the increase in CTI were nearly identical between occurrence and abundance-weighted CTI; however, changes in occurrence CTI were marginally smaller (0.78 ± 1.75 °C). The global model, which quantified the change in CTI as a function of space, time, and changes in short-, medium-, and long-term temperature increases, explained a substantial portion of the deviance in both the abundance-weighted (Table S1; 86.0%, adj-R^2 = 0.849) and occurrence models (Table S1; 86.3%, adj-R^2 = 0.851).

The results of our analysis were consistent irrespective of the grid scale used in aggregating communities (Figure S2; Table S2). The exception was in areas of British Columbia and Alaska where a highly concentrated spatial pattern of bumble bee records likely led to a predicted decrease in CTI in grid cells when aggregated at the 50 and 25 km grid scale. Aggregating at the largest scale (100 km center-to-side hexagonal grid) revealed the most wide-spread increases in CTI, with nearly all grid cells exhibiting an increase in CTI from 1989 to 2018.

Our models performed well when cross-validated using withheld data from the BBNA database (Figure S3). Coefficient of determination (R^2) values ranged from 0.79-0.81; root mean squared error (RMSE) ranged from 1.22-1.31; and mean absolute error (MAE) ranged from 0.91-0.96. In addition, our model performance was consistent across the three tested grid scales. Predictions were most accurate for CTI values ranging from 23-28°C which corresponded to the regions where the bulk of the occurrence records were collected. Prediction accuracy was most variable among cool regions in the north and sub-arctic (CTI < 23°C).

Shifts in CTI are strongly related to long-term increases in summer temperature

Summertime maximum temperatures have increased by 1989-2018 (Fig. 2C-E), with increases most apparent at 10- (0.630 ± 0.405 °C) and 30-year average anomalies (0.969 ± 0.342°C; Figure 1D, E; Figure S4). Increases in the 30-year summertime maximum temperature anomaly showed a strong statistical association with increases in bumble bee CTI (Figure 2C; F = 4.561, p = 0.002). Increases in the 30-year temperature anomaly between 0-0.5°C had no impact on CTI. However, increases of over 0.5°C were associated with a rapid increase of up to 1°C in bumble bee CTI (partial effect due solely to 30-year temperature anomaly). Beyond a 1°C change in the 30-year temperature anomaly the changes in CTI rapidly increase, with gains of 1 to 6.8°C. The relationship of CTI with short term, 3-year moving average shifts in summer temperature anomalies, while statistically supported, was weak and variable over the range of the anomalies (Figure 3A; F = 2.584, p

= 0.032). There was no statistically supported relationship between the 10-year average anomaly and bumble bee CTI (Figure 3B; F = 0.064, p = 0.802).

CTI is increasing fastest at low and high elevations, high latitudes, and more recent years

We examined patterns in the rate of change in CTI across the continent to determine where and when the most extreme changes in CTI were occurring and whether these areas overlapped with areas known to be heavily impacted by a warming climate (Janousek et al., 2023). The rate of change in CTI was greatest at low (< 800 m) and high elevations (> 2000 m; Figure 5A) and increased with increasing latitude (Figure 5B). CTI increases predicted at high elevations also had greater uncertainty than those at low elevations, due in part to a higher concentration of occurrence records at lower elevations. Moreover, the rate of change in CTI has increased from 1989-2018, with CTI increasing most rapidly after 2010 (Figure 5C). These results varied slightly when analyzed with predictions from only grid cells containing occurrence records, with changes in CTI being greatest at high elevations (Figure S5A; > 2000 m) and mid-high latitudes (Figure S5B; 35 – 60°). The temporal patterns of the rate of change were largely similar but were positive only from 2003 and beyond (Figure S5C), confirming the accelerating rate of CTI change from 2010 onward that is exhibited when using predictions from all grid cells (Figure 5C).

CTI changes driven by loss of cool-adapted and increase in warm-adapted species

In the model predicting the temporal trend coefficient for species relative abundance, there was a significant interaction between species thermal niche, latitude, and propagated error ($\chi^2 = 14.53$, $p < 0.001$, Table S3). The relative abundance of cool-adapted species has declined across North America, with the rate of decrease (i.e., binomial model coefficient estimates) lowest at high latitudes (Figure 6). In contrast, the relative abundance of warm-adapted species has increased across all areas south of ~50° latitude. Beyond this 50° parallel, warm-adapted species are also decreasing in relative abundance. This general trend, a consistent loss of cold-adapted species and increase in warm-adapted species across most latitudes was broadly consistent across ecological regions (Figure S6).

Discussion

We documented significant, rapid spatially extensive shifts in the thermal composition of North American bumble bee communities in response to long-term increases in summer temperatures. Over the last 29 years across the continent, bumble bee community assemblages increasingly consist of fewer cool-adapted and more warm-adapted species with resultant increases in the community temperature index, a measure of the balance of warm- and cool-adapted species, most pronounced at mid- to high latitudes, and high elevations in the American Rockies, Intermountain West, and central Mexico. We also document an alarming trend suggesting that above 50°N, both cool- and warm-adapted species are declining in relative abundance, indicating that warming temperatures are outpacing the capacity of bumble bee species to respond or adapt (Kerr et al., 2015). The community temperature index increased according to both occurrence and abundance-weighted indices, suggesting that shifts in both local abundance (i.e., loss of cool-adapted species) and broader changes in species occurrence (i.e., range shifts) underlie the observed changes in community composition. Our model results are consistent with occupancy patterns that reveal both winners and losers among bumble bee species in response to anthropogenic climate change (Jackson et al., 2022). Overall, our work provides strong evidence of the pervasive impacts a warming planet has for insect biodiversity, particularly for historically cool-adapted species, and identifies regions of concern where anthropogenic climate warming is rapidly restructuring the communities of an ecologically important group of insects.

An increase in species turnover within biological communities is a logical consequence of a rapidly warming climate (Tingley & Beissinger, 2013). Similar shifts in community composition have been observed in bird communities in response to both warming summer (Devictor et al., 2008, 2012) and winter (Princé & Zuckerberg, 2015) temperatures. Because insects are ectotherms, temperature-induced shifts in range and abundance may be even more pronounced. Indeed, large changes in insect CTI have been observed for both bumble bees (Fourcade et al., 2019) and butterflies (Devictor et al., 2012); however, trends in CTI are often not explicitly tied to spatial and temporal patterns of warming temperatures. Our results explicitly link these two phenomena – revealing a clear statistical relationship between increases in CTI and long-term increases in maximum summer temperatures across North America. Areas experiencing a 30-year temperature anomaly of greater than or equal to 0.5°C strongly associated with a rapid increase in bumble bee CTI (Figure 2; dark orange and red areas). It is worth noting that the historical baseline period we choose for calculating species STI values is due to the availability of interpolated climate data. Choosing an earlier baseline period could reveal different patterns in community change, however this is unlikely given the stability of summer temperatures relative to the dramatic increases observed in recent decades.

The frontline of species' responses to climate have tended to be at high latitudes. Northern regions have experienced rapid increases in temperature leading to pronounced phenological shifts across taxa (Parmesan, 2007). Our results support this trend, finding greatest rates of bumble bee CTI change at higher latitudes and high elevation. The bumble bee species in these locations tend to have narrower ranges and be cold-adapted, traits identical to other insect taxa that have exhibited declines due to climate (Engelhardt et al.,

2022; Halsch et al., 2021; Neff et al., 2022). Alarmingly, our results found that even warm-adapted species are struggling to respond to the pace of warming temperatures at higher latitudes (CITE). We found that both cool- and warm-adapted bumble bee species north of 50°N have exhibited significant declines in relative abundance. This result supports previous work describing the limited capacity of bumble bees to track their northern range limits in accordance with warming temperatures (Kerr et al., 2015). Though additional confirmation is needed, our results suggest that northern bumble bee communities are in crisis, with significant species turnover and declines in abundance that may threaten the persistence of populations in the coming decades.

Rapidly increasing CTI at high elevations suggests that cold-adapted species are being displaced by warm-adapted, low-elevation species. This phenomenon has been observed in the US Rocky Mountains where bumble bee communities are increasingly dominated by low-elevation species using high-elevation habitats as a thermal refugia (Miller-Struttmann et al., 2022). An upslope range expansion appears to be a common response of bumble bee communities to warming temperatures rather than expansions of northern ranges (Kerr et al., 2015; Sirois-Delisle & Kerr, 2018). Despite the rapid changes observed at higher latitudes, biological communities in southern latitudes and lower elevations are not protected from a changing climate (Dillon et al., 2010), and we documented some shifts in CTI in central Mexico and at low elevations. That said, if species lost from communities have STI values comparable to those species remaining, shifts in CTI and community composition may be effectively masked, highlighting a limitation of our approach.

An increase in CTI could be the result of two mechanisms. First, shifts in the occurrence of bees within a community (i.e., immigration/extirpation of warm-/cool-adapted species via range expansion/contraction) and second, changes in the local abundance of warm-/cool-adapted species. We found evidence supporting both mechanisms by modeling occurrence and abundance-weighted measures of CTI. Shifts in local relative abundance align with existing research (Cameron et al., 2011; J. Hemberger et al., 2021); however, substantial range expansion of warm-adapted bumble bees has not been described (Kerr et al., 2015) and may be unlikely given bumble bee dispersal capacities (Fijen, 2021). That said, select species of bumble bees may be capable of long-distance dispersal (Fijen, 2021), and significant range shifts in other insect taxa have been observed (Warren et al., 2001; Hinckling.2005). Regardless, our thermal niche analysis revealed there are a host of warm-adapted species whose relative abundance is increasing significantly. This result indicates that certain species are sensitive to and more capable of effectively tracking/adapting to ideal climatic conditions (Maebe et al., 2021). Indeed, several bumble bee species have exhibited both range increases (Looney et al., 2019; e.g., B. impatiens Palmier et al., 2019) and increases in local abundance. However, other species (e.g., *B. occidentalis*) are not able to successfully track warming and are likely to suffer substantial reductions in range as a result (Janousek et al., 2023). Moreover, our analysis found that, north of the US/Canadian border, even warm-adapted species are at risk, with negative trends in species' relative abundance. Such contrasts highlight the species-specific nature of bumble bee responses to a rapidly changing climate (Jackson et al., 2022; Whitehorn et al., 2022). Additional research is needed detailing species-specific responses to warming conditions – focusing on identifying the physiological and evolutionary mechanisms that drive species' plasticity to changing environmental conditions.

An increase in the occurrence and abundance of warm adapted species does suggest a physiological/climate preference mechanism is at play (i.e., direct effect). Several studies document significant, direct effects of warming on insect pollinators (CaraDonna et al., 2018; Hemberger et al., 2023; Kenna et al., 2021), however indirect effects mediated through biotic interactions may be just as if not more important (Ockendon et al., 2014, but see Iler et al., 2021). In the context of our study, such indirect effects imply that shifts in bumble bee community composition are occurring in part in response to climate-induced changes in the resource landscape (i.e., indirect effects). For example, warming climates can widen the temporal availability of resources due to earlier snowmelts, which in turn lead to an increase in bumble bee abundance (Ogilvie et al., 2017). Warming may also create phenological mismatches that reduce available forage for bees (Pyke et al. 2016, but see Bartomeus et al., 2011). Similarly, an increase in hot, dry summer conditions can significantly reduce floral resources and the bumble bees that depend on them (Iserbyt & Rasmont, 2013), and similar patterns have been observed for butterflies (Crossley et al., 2021). Unfavorable conditions, often a result of extreme weather events such as heat waves and droughts, can create resource bottlenecks that have the potential to lead to population declines and local extirpation (Maron et al., 2015). Heat waves, for example, are expected to increase significantly in the coming century (Lopez et al., 2018; Meehl & Tebaldi, 2004; Thompson et al., 2022). Because our study could not differentiate between direct and indirect pathways, parsing their relative impacts on bumble bees and other taxa is a critical research need. In the meantime, supporting bumble bees in the face of both direct and indirect effects may be accomplished by maintaining climate refugia, such as heterogeneity in vegetation structure, that can provide microclimatic respite from temperature extremes to bees (Pincebourde & Woods, 2020) and other taxa (e.g., birds, Kim et al., 2022) in addition to increasing spatial/temporal resource continuity to minimize negative indirect effects (Maron et al., 2015).

Given the spatiotemporal extent of our study, it is likely that warming summer temperatures and the temperature profile of a given bumble bee assemblage may co-vary with other, known factors of bumble bee community composition and occurrence. For example, losses in certain species across their range may be linked to disease (Szabo et al., 2012). Additionally, at large-scales, a loss of suitable habitat via land-use intensification and change is also of concern. However, when examined together with shifts in land-use, climatic variables (and their associated indirect effects) tend to have as much or more power to explain long-term species trends than land-use or resource availability in bumble bees (Kerr et al. 2015) and other wild bee species (Duchenne et al., 2020). Moreover, the areas of greatest increase in CTI are in areas removed from the most significant effects of land-use change (e.g., high latitudes and elevations; Halsch et al., 2021). Regardless, managing habitat offers a critical tool that can be used to mitigate the impacts of a changing climate (Kim et al., 2022; Oliver et al., 2016; Oliver et al., 2015; Outhwaite et al., 2022).

Conclusions

Climate change is poised to have significant, cross-scale impacts on insect behavior, populations, and communities (Halsch et al., 2021; Høye et al., 2021; Lehmann et al., 2020; Raven & Wagner, 2021). In this paper, we document a substantial shift in the functional composition of bumble bee communities with respect to climate that is tied to a long-term

increase of summer temperatures in North America. Due to changes in both occurrence and abundance, several species appear to be tracking climate warming, however we found that cold-adapted species appear lack the adaptive capacity to cope with rapidly climbing temperatures and are being lost from bumble bee communities across the continent. Although the exact mechanisms of these community-level shifts remain unknown (i.e., direct vs. indirect effect of warming), our work adds to a growing body of evidence that suggests climate change is having a significant, negative impact on many species with unknown consequences for ecosystems. It is critical that we focus on designing adaptation measures, such as climate refugia and climate-focused habitat conservation, to help combat the ongoing direct and indirect impacts a rapidly warming planet threatens. However, such efforts will only be successful in conjunction with substantial decreases in emissions (Oliver et al., 2015) – an essential solution to safeguard the planet's biodiversity for generations to come.

Acknowledgements

Special thanks to Rachel Winfree for comments on an earlier draft of this manuscript. This project was funded by a USDA NIFA Postdoctoral Fellowship to JH (Award No. 2020-67034-31944)

Data access

All data and R code for analyses, figures, and manuscript are available on FigShare (https://figshare.com/s/59aa9a55ab5bafb65901) and will be made public upon publication.

Figures and Tables

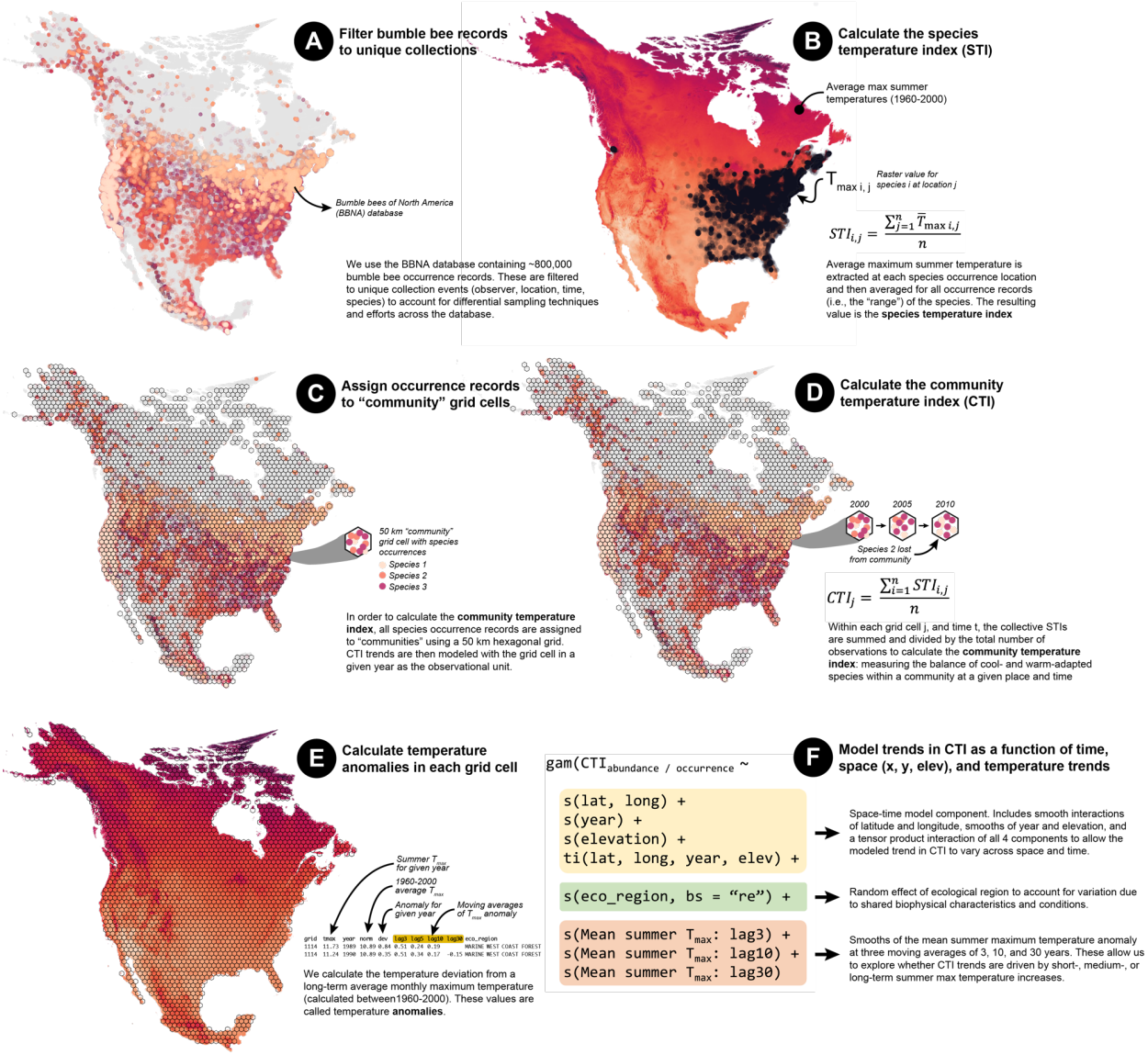

Figure 1: Conceptual figure of data cleaning (A), STI calculation (B), community assignment (C), CTI calculation (D), temperature anomaly calculations (E) and modeling procedures used in our analyses (F).

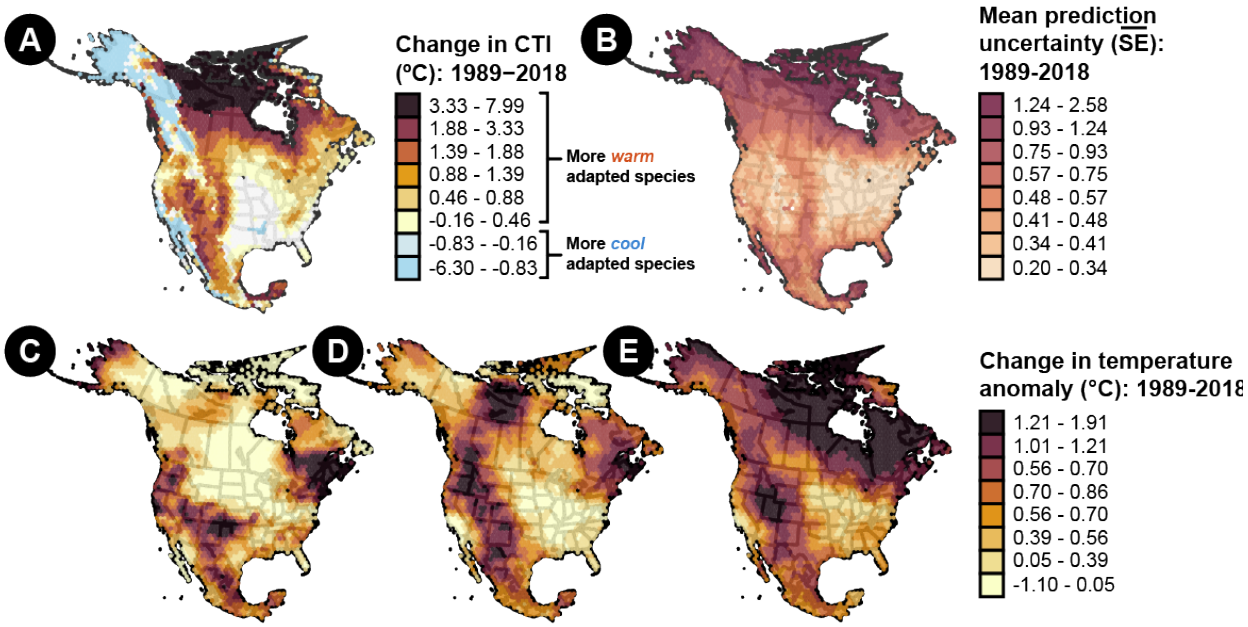

Figure 2: (A) Extrapolated spatial projection of the estimated change in community temperature index from 1990-2018 across North America. Differences in CTI were calculated for each grid cell by subtracting the model predicted CTIt = 1989 from predicted CTIt = 2018. (B) Spatial projection of the mean uncertainty estimates across years from 1989-2018. (C) Spatial projection of the change in the 3-year, 10-year (D) and 30-year (E) average temperature anomaly. Differences were calculated by subtracting the 1989 anomaly from the 2018 anomaly for each grid cell. Hexagonal grid cells are 100 km from side to side (~8600 km2).

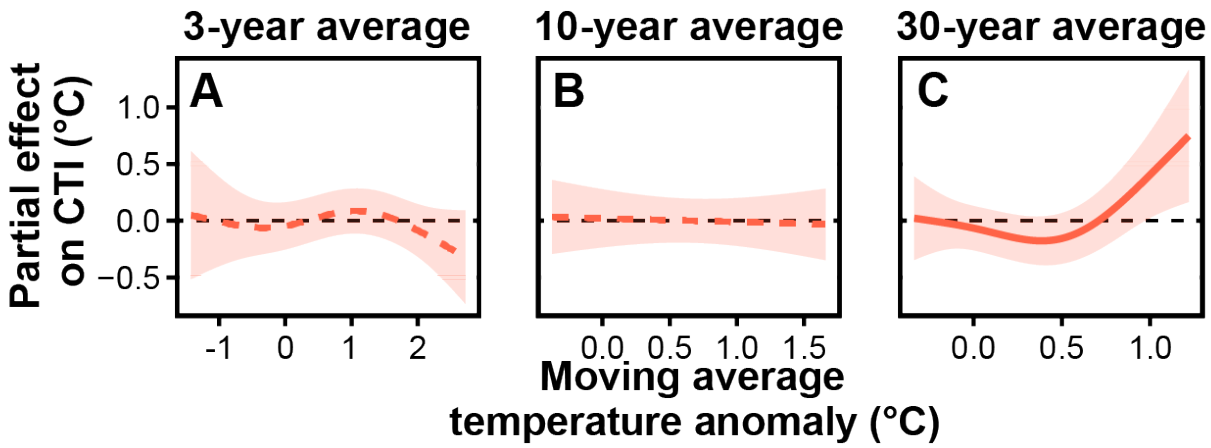

Figure 3: Generalized additive model partial plots (i.e., marginal effects) show the model predicted effect of (A) 3, (B) 10, and (C) 30-year moving average temperature anomalies on the community temperature index. Positive values on the y-axes indicate an increase in CTI, while positive values on the x-axes indicate an increase in the average temperature relative to the long-term average. Solid line indicates strong evidence of a relationship.

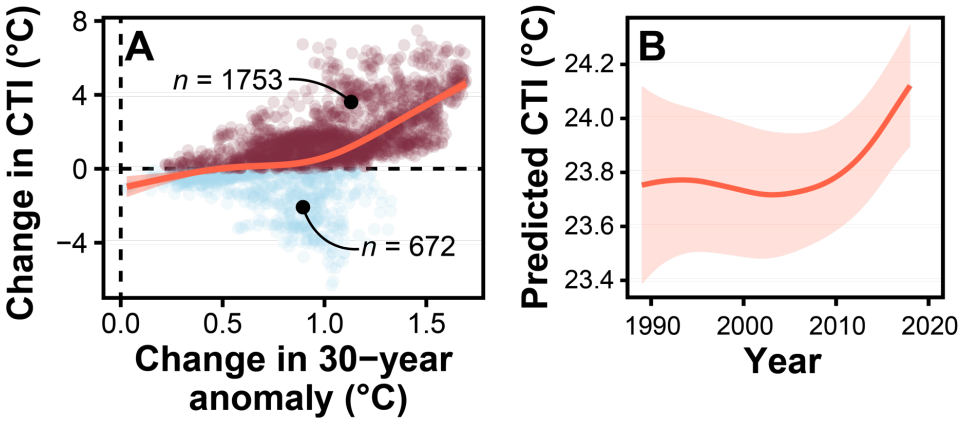

Figure 4: A significant increase in bumble bee CTI is strongly associated with long-term warming and has accelerated in the last 15 years. (A) Biplot of change in 30-year temperature anomaly and change in bumble bee CTI for each grid cell across North America. Trendline is a GAM fit including the 95% confidence interval. Dashed lines indicate no change in anomaly or CTI for the X and Y axes, respectively. (B) Model estimated temporal trend in CTI across North America. Yearly predictions are calculated from the global model for each grid cell, and the trend within each region is illustrated with a GAM fit including the 95% confidence interval.

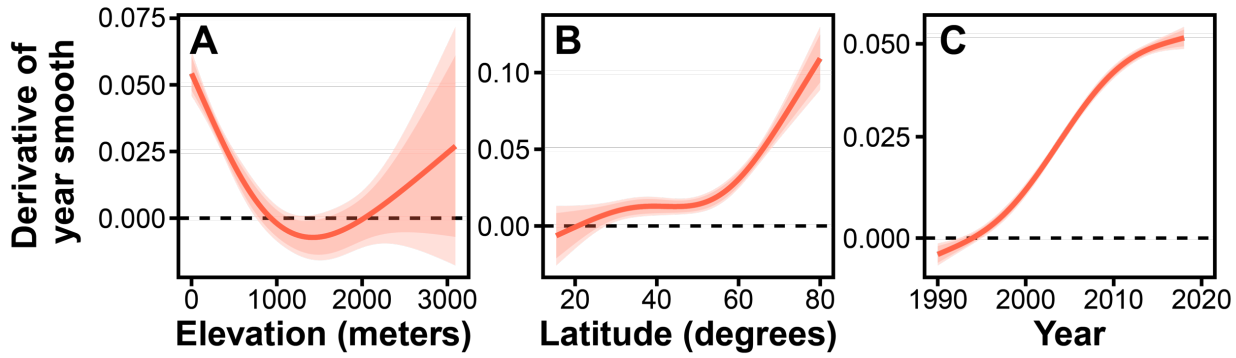

Figure 5: Estimates of the rate of change in CTI over time across (A) elevation, (B) latitude, and (C) year. Yearly predictions of CTI are calculated from the global model for each grid cell using a generalized additive model with a single smooth of year to determine the temporal trend in CTI within the grid cell. For each fitted smooth (except for the year, C), we then calculated the mean derivative across its range (1989-2018) for each grid cell. We then plotted these derivative estimates against elevation and latitude to explore, across the extent of North America, where the rate CTI change is greatest. We visualized the relationships (red lines) using a simple GAM. Model fits include the 95% confidence interval. # References

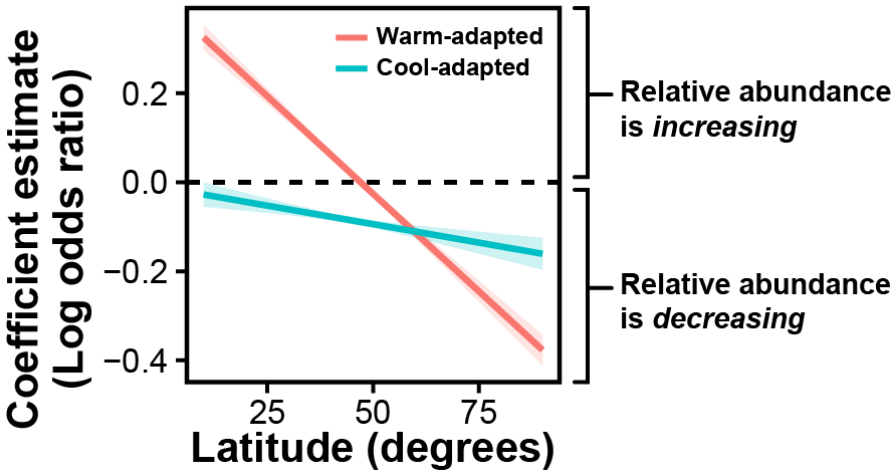

Figure 6: Marginal effect plots describing predicted coefficients for the temporal trend in warm- and cool-adapted species relative abundance across latitude in North America (± 95% CI). Values above zero indicate an increase in relative abundance from 1989-2018, while values below zero indicate a decrease.

Supplementary Materials

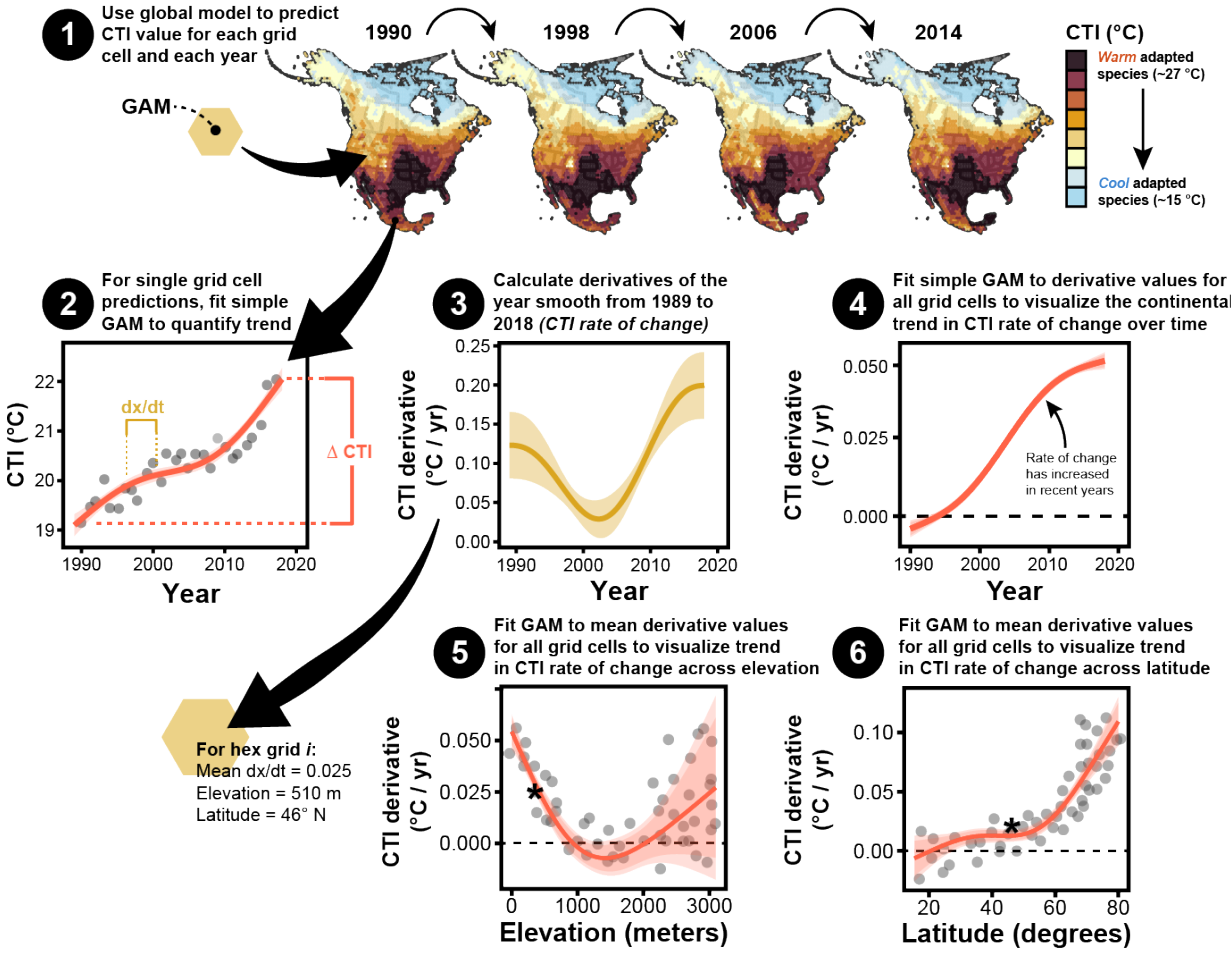

Figure S1: Conceptual diagram of the derivative calculations conducted to determine whether the rate of increase (i.e., derivative) of bumble bee CTI has remained steady or accelerated over space and time. (1) We use the global model to predict the CTI in each grid cell for each year of the study, from 1989-2018. (2) For each grid cell, we fit a GAM through the predicted points to visualize and quantify the trend in CTI from 1989-2018. From these data, we also calculated the change in CTI from 1989-2018 (change in CTI) which is plotted in Fig. 1A. The overall change, however, tells us nothing of the functional form of the relationship between CTI and time, elevation, etc. To address this, we calculated the first derivative across the fitted smooth to determine how the rate of change in CTI varied across time, elevation, and latitude (Fig. 2). (3) For each grid cell's fitted GAM, we calculated the derivative of the year smooth at a range of values between 1989-2018. In this example, because CTI is increasing throughout the entire study period, the derivative is > 0 at all years. (4) We then took the derivative estimates for all grid cells and fit a GAM to visualize the trend between the derivative and time. For elevation (5) and latitude (6), we first averaged the derivative value from 1989-2018 to determine the mean slope for each grid cell before plotting that against the mean elevation and latitude of each grid cell and visualizing the relationship with a GAM. Transparent points are illustrative (not actual

601 values) of individual hex grid derivative values across the range of elevation and latitude.
602 The black star represents a hypothetical mean derivative value from the example plot in
603 (3) to illustrate how mean derivative values are used to assess the trend.

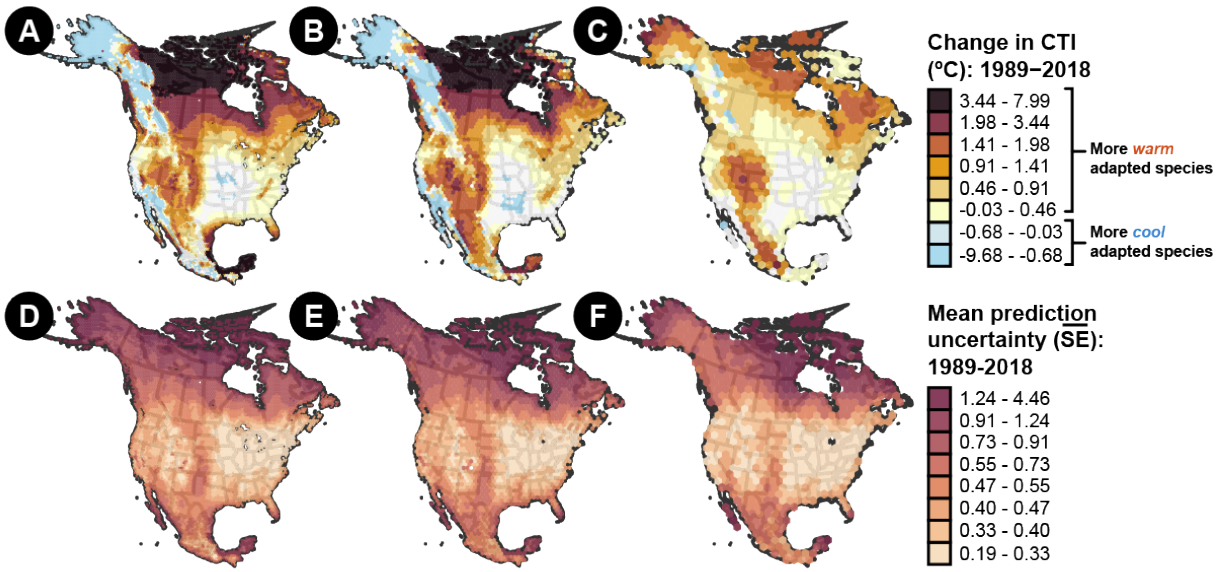

Figure S2: Predicted change in bumble bee CTI across North America between 1989-2018 at three different spatial resolutions of hexagonal grid (distance indicates side-to-side): (A) 50 km; (B) 100 km; (C) 200 km; along with the mean prediction uncertainty at the same resolutions.

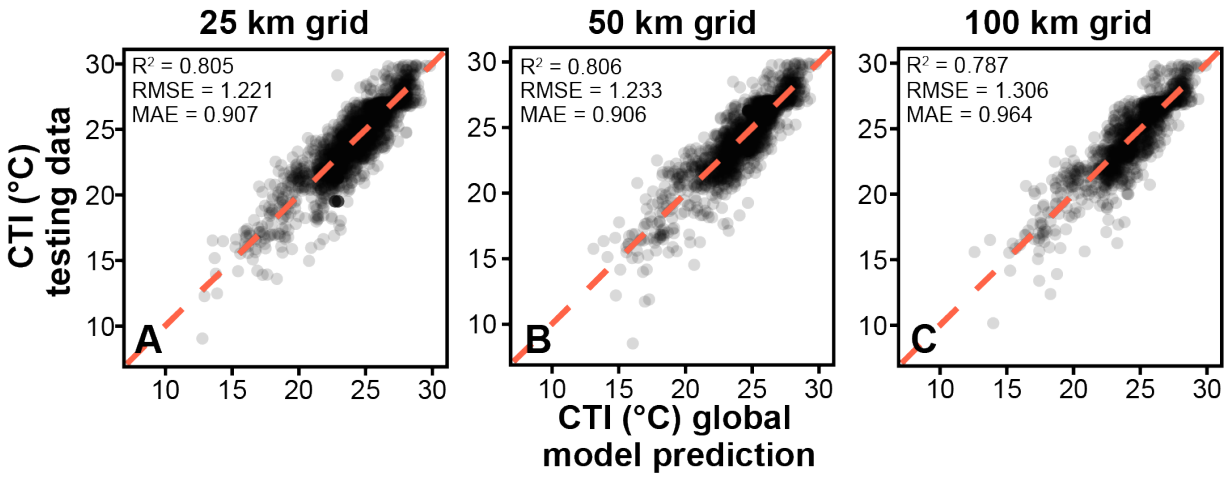

Figure S3: Abundance-weighted global model cross validation results at three different scales of (A) 25 km, (B) 50 km, and (C) 100 km center-to-edge hexagonal grids. Cross validation metrics are given in the top left of each panel including coefficient of determination (R2), root mean squared error (RMSE), and mean absolute error (MAE).

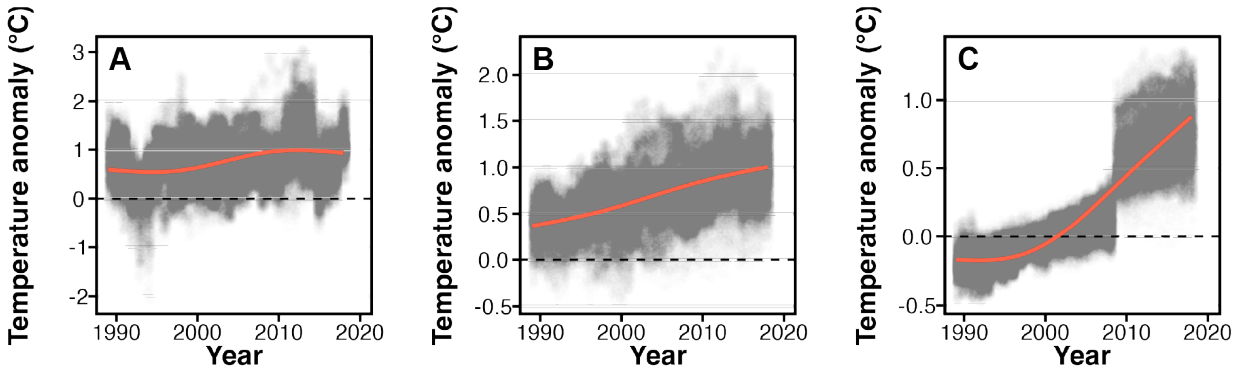

Figure S4: Trend in summer (June – September) maximum temperature anomalies at (A) 3-year, (B) 10-year, and (C) 30-year moving averages. Transparent points are raw values and red lines are GAM trendlines.

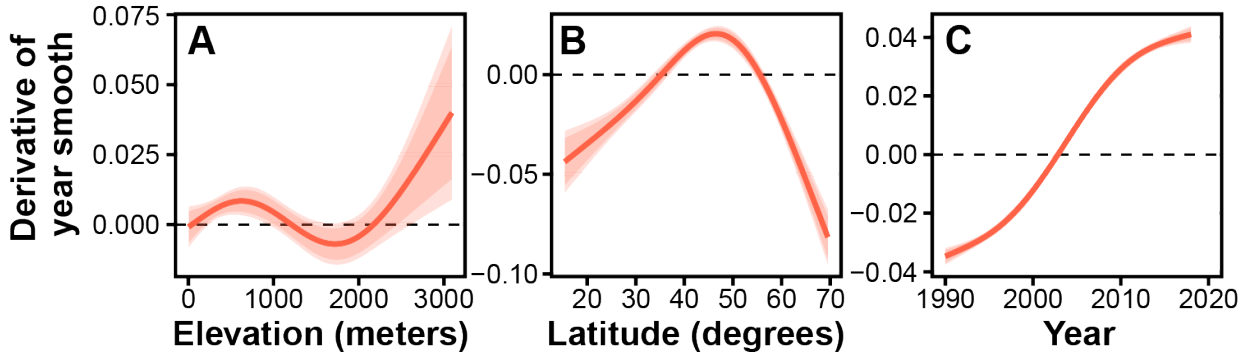

Figure S5: Estimates of the rate of change in CTI over time across (A) elevation, (B) latitude, and (C) year using predictions only from grid cells containing occurrence records (conservative approach). Yearly predictions are calculated from the global model for each grid cell using simple generalized additive models with a single smooth of year to determine CTI trend within the grid cell. For each fitted smooth (except for the year, C), we then calculated the mean derivative across its range (1989-2018) for each grid cell. We then plotted these derivative estimates to explore, across the extent of North America, whether increases in CTI were varied with elevation or over time. We calculated predictions (red lines) from a generalized additive model using a thin-plate basis function and 3 knots for visual purposes only. Estimates include the 95% confidence interval.

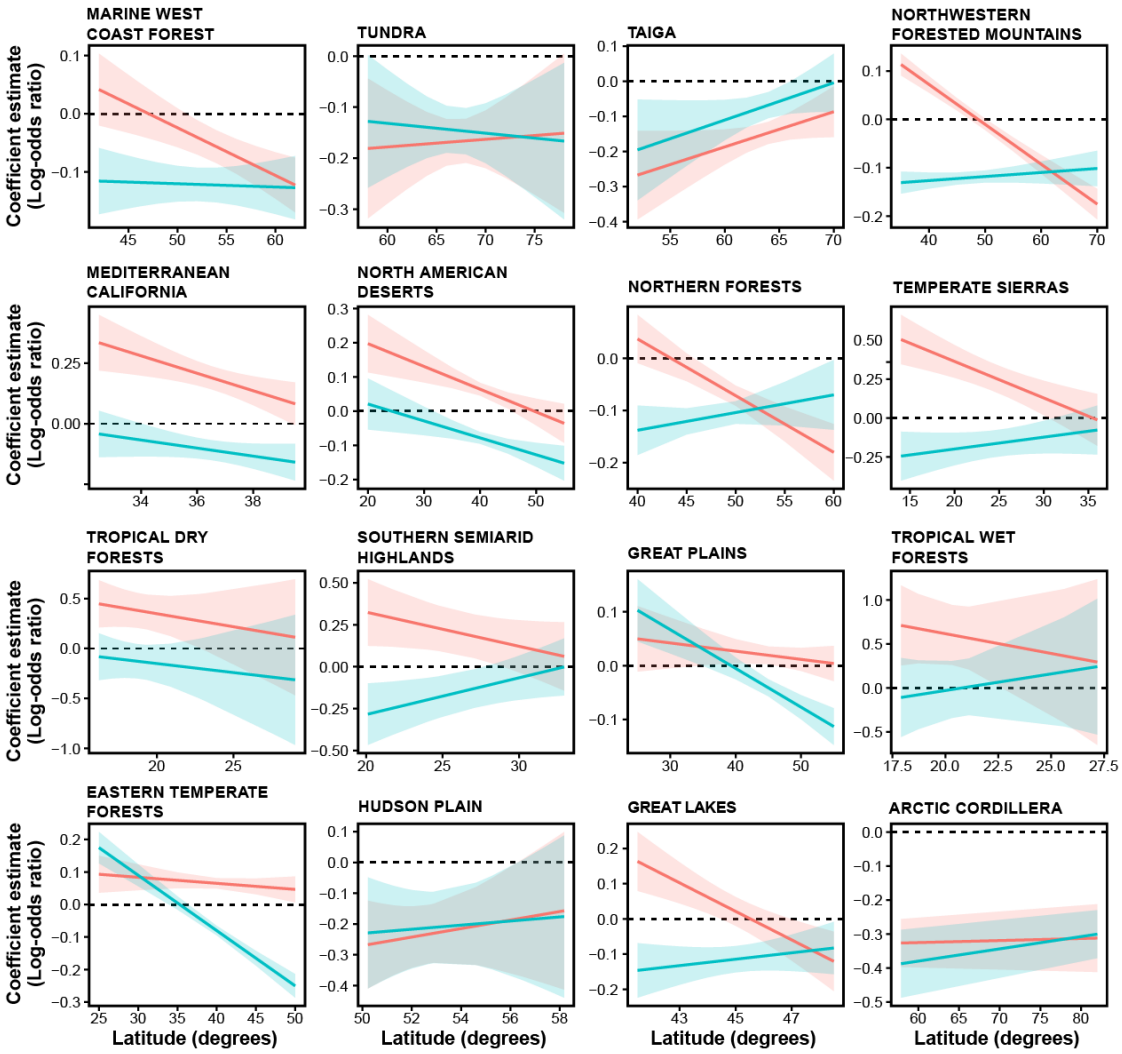

Figure S6: Marginal effect plots describing predicted coefficients for the temporal trend in warm- and cool-adapted species relative abundance across latitude in North America (± 95% CI) for each ecological region. Values above zero indicate an increase in relative abundance from 1989-2018, while values below zero indicate a decrease.

Table S1: Results from a generalized additive model for CTI using occurrence-only and abundance-weighted records from 1989-2018.

	Occurrence model			Abundance model		
Model smooth	**EDF**	**F**	**p value**	**EDF**	**F**	**p value**
Latitude, longitude	282.065	16.778	< 0.001	270.546	18.099	< 0.001
Year	2.945	4.015	0.004	2.353	3.592	0.022
Elevation	7.995	23.926	< 0.001	7.615	25.782	< 0.001
Latitude, longitude, elevation, year	100.149	3.782	< 0.001	97.853	2.996	< 0.001
Ecological region	10.526	2.388	< 0.001	9.855	1.644	< 0.001
Mean Tmax 3-year MA	2.968	2.584	0.032	2.827	2.500	0.039
Mean Tmax 10-year MA	1.002	0.064	0.803	1.001	0.475	0.491
Mean Tmax 30-year MA	2.967	4.561	0.002	3.377	6.712	< 0.001
Model n	5273			5273		
Deviance explained	0.860			0.863		
R-squared (adjusted)	0.849			0.851		

*EDF :estimated degrees of freedom (i.e., smooth wiggliness)

637 **Table S2:** Results from a generalized additive model for CTI using occurrence-only records
638 at three different spatial resolutions (community grid scale) at 25, 50, and 100 km from
639 1989-2018.

	25 km grid scale			50 km grid scale			100 km grid scale		
Model smooth	**EDF**	**F**	**p value**	**EDF**	**F**	**p value**	**EDF**	**F**	**p value**
Latitude, longitude	294.224	18.839	< 0.001	270.546	18.099	< 0.001	181.650	17.769	< 0.001
Year	3.653	5.293	< 0.001	2.353	3.592	0.022	2.538	1.609	0.164
Elevation	9.360	34.646	< 0.001	7.615	25.782	< 0.001	1.000	52.860	< 0.001
Latitude, longitude, elevation, year	106.844	4.744	< 0.001	97.853	2.996	< 0.001	51.223	2.558	< 0.001
Ecological region	10.889	4.824	< 0.001	9.855	1.644	< 0.001	11.650	4.843	< 0.001
Mean Tmax 3-year MA	2.881	3.999	0.008	2.827	2.500	0.039	1.000	0.041	0.840
Mean Tmax 10-year MA	1.000	0.061	0.805	1.001	0.475	0.491	3.511	5.344	0.004
Mean Tmax 30-year MA	2.919	5.177	0.001	3.377	6.712	< 0.001	3.029	4.430	0.003
Model n	7582			5273			3078		
Deviance explained	0.840			0.860			0.862		
R-squared (adjusted)	0.831			0.849			0.850		

640 *EDF :estimated degrees of freedom (i.e., smooth wiggliness)

641

642 **Table S3:** Type III Wald Chi-squared effect test results from a generalized linear model for
643 the temporal trend in species relative abundance for two thermal niche groups: cool- and
644 warm-adapted.

Model term	**Model coefficient**	$\chi 2$	**Degrees of freedom**	***p*-value**
Thermal niche	0.497	506.26	1	< 0.001
Latitude	-0.002	461.18	1	< 0.001
Error propagation	-0.005	20.14	1	< 0.001
Thermal niche * latitude	-0.008	191.57	1	< 0.001
Thermal Niche * error	-0.059	67.62	1	< 0.001
Latitude * error	0.0004	54.51	1	< 0.001
Thermal niche * latitude * error	0.001	14.53	1	< 0.001

645

References

Bartomeus, I., Ascher, J. S., Wagner, D., Danforth, B. N., Colla, S., Kornbluth, S., & Winfree, R. (2011). Climate-associated phenological advances in bee pollinators and bee-pollinated plants. *Proceedings of the National Academy of Sciences*, *108*(51), 20645–20649. https://doi.org/10.1073/pnas.1115559108

Bartomeus, I., Stavert, J. R., Ward, D., & Aguado, O. (2019). Historical collections as a tool for assessing the global pollination crisis. *Philosophical Transactions of the Royal Society B*, *374*(1763), 20170389. https://doi.org/10.1098/rstb.2017.0389

Birch, C. P. D., Oom, S. P., & Beecham, J. A. (2007). Rectangular and hexagonal grids used for observation, experiment and simulation in ecology. *Ecological Modelling*, *206*(3-4), 347–359. https://doi.org/10.1016/j.ecolmodel.2007.03.041

Cameron, S. A., Lozier, J. D., Strange, J. P., Koch, J. B., Cordes, N., Solter, L. F., & Griswold, T. L. (2011). Patterns of widespread decline in North American bumble bees. *Proceedings of the National Academy of Sciences*, *108*(2), 662–667. https://doi.org/10.1073/pnas.1014743108

CaraDonna, P. J., Cunningham, J. L., & Iler, A. M. (2018). Experimental warming in the field delays phenology and reduces body mass, fat content and survival: Implications for the persistence of a pollinator under climate change. *Functional Ecology*, *32*(10), 2345–2356. https://doi.org/10.1111/1365-2435.13151

Colla, S. R., Otterstatter, M. C., Gegear, R. J., & Thomson, J. D. (2006). Plight of the bumble bee: Pathogen spillover from commercial to wild populations. *Biological Conservation*, *129*(4), 461–467. https://doi.org/10.1016/j.biocon.2005.11.013

Crossley, M. S., Smith, O. M., Berry, L. L., Phillips-Cosio, R., Glassberg, J., Holman, K. M., Holmquest, J. G., Meier, A. R., Varriano, S. A., McClung, M. R., Moran, M. D., & Snyder, W. E. (2021). Recent climate change is creating hotspots of butterfly increase and decline across North America. *Global Change Biology*, *27*(12), 2702–2714. https://doi.org/10.1111/gcb.15582

Daniel Baston. (2022). *Exactextractr: Fast extraction from raster datasets using polygons*. https://CRAN.R-project.org/package=exactextractr

Devictor, V., Julliard, R., Couvet, D., & Jiguet, F. (2008). Birds are tracking climate warming, but not fast enough. *Proceedings of the Royal Society B: Biological Sciences*, *275*(1652), 2743–2748. https://doi.org/10.1098/rspb.2008.0878

Devictor, V., Swaay, C. van, Brereton, T., Brotons, L., Chamberlain, D., Heliölä, J., Herrando, S., Julliard, R., Kuussaari, M., Lindström, Å., Reif, J., Roy, D. B., Schweiger, O., Settele, J., Stefanescu, C., Strien, A. V., Turnhout, C. V., Vermouzek, Z., WallisDeVries, M., … Jiguet, F. (2012). Differences in the climatic debts of birds and butterflies at a continental scale. *Nature Climate Change*, *2*(2), 121–124. https://doi.org/10.1038/nclimate1347

Dillon, M. E., Wang, G., & Huey, R. B. (2010). Global metabolic impacts of recent climate warming. *Nature*, *467*(7316), 704–706. https://doi.org/10.1038/nature09407

685 Dowle, M., & Srinivasan, A. (2023). *Data.table: Extension of 'data.frame'*. https://CRAN.R-
686 project.org/package=data.table

687 Duchenne, F., Thébault, E., Michez, D., Gérard, M., Devaux, C., Rasmont, P., Vereecken, N. J., &
688 Fontaine, C. (2020). Long-term effects of global change on occupancy and flight period of
689 wild bees in Belgium. *Global Change Biology*. https://doi.org/10.1111/gcb.15379

690 Engelhardt, E. K., Biber, M. F., Dolek, M., Fartmann, T., Hochkirch, A., Leidinger, J., Löffler, F.,
691 Pinkert, S., Poniatowski, D., Voith, J., Winterholler, M., Zeuss, D., Bowler, D. E., & Hof, C.
692 (2022). Consistent signals of a warming climate in occupancy changes of three insect taxa
693 over 40 years in central Europe. *Global Change Biology*, *28*(13), 3998–4012.
694 https://doi.org/10.1111/gcb.16200

695 Fick, S. E., & Hijmans, R. J. (2017). WorldClim 2: new 1km spatial resolution climate
696 surfaces for global land areas. *International Journal of Climatology*, *12*(37), 4302–4315.
697 https://doi.org/10.1111/gcb.15379

698 Fijen, T. P. M. (2021). Mass-migrating bumblebees: An overlooked phenomenon with
699 potential far-reaching implications for bumblebee conservation. *Journal of Applied Ecology*,
700 *58*(2), 274–280. https://doi.org/10.1111/1365-2664.13768

701 Firke, S. (2021). *Janitor: Simple tools for examining and cleaning dirty data*. https://CRAN.R-
702 project.org/package=janitor

703 Fourcade, Y., Åström, S., & Öckinger, E. (2019). Climate and land-cover change alter
704 bumblebee species richness and community composition in subalpine areas. *Biodiversity*
705 *and Conservation*, *28*(3), 639–653. https://doi.org/10.1007/s10531-018-1680-1

706 Gotelli, N. J., Booher, D. B., Urban, M. C., Ulrich, W., Suarez, A. V., Skelly, D. K., Russell, D. J.,
707 Rowe, R. J., Rothendler, M., Rios, N., Rehan, S. M., Ni, G., Moreau, C. S., Magurran, A. E., Jones,
708 F. A. M., Graves, G. R., Fiera, C., Burkhardt, U., & Primack, R. B. (2021). Estimating species
709 relative abundances from museum records. *Methods in Ecology and Evolution*.
710 https://doi.org/10.1111/2041-210x.13705

711 Guzman, L. M., Johnson, S. A., Mooers, A. O., & M'Gonigle, L. K. (2021). Using historical data
712 to estimate bumble bee occurrence: Variable trends across species provide little support
713 for community-level declines. *Biological Conservation*, *257*, 109141.
714 https://doi.org/10.1016/j.biocon.2021.109141

715 Halsch, C. A., Shapiro, A. M., Fordyce, J. A., Nice, C. C., Thorne, J. H., Waetjen, D. P., & Forister,
716 M. L. (2021). Insects and recent climate change. *Proceedings of the National Academy of*
717 *Sciences*, *118*(2), e2002543117. https://doi.org/10.1073/pnas.2002543117

718 Hartig, F. (2022). *DHARMa: Residual diagnostics for hierarchical (multi-level / mixed)*
719 *regression models*. https://CRAN.R-project.org/package=DHARMa

720 Hemberger, J. A., Rosenberger, N. M., & Williams, N. M. (2023). Experimental heatwaves
721 disrupt bumblebee foraging through direct heat effects and reduced nectar production.
722 *Functional Ecology*, *37*(3), 591–601. https://doi.org/10.1111/1365-2435.14241

Hemberger, J., Crossley, M. S., & Gratton, C. (2021). Historical decrease in agricultural landscape diversity is associated with shifts in bumble bee species occurrence. *Ecology Letters*, *24*(9), 1800–1813. https://doi.org/10.1111/ele.13786

Hijmans, R. J. (2023). *Raster: Geographic data analysis and modeling*. https://CRAN.R-project.org/package=raster

Hoover, S. E. R., Ladley, J. J., Shchepetkina, A. A., Tisch, M., Gieseg, S. P., & Tylianakis, J. M. (2012). Warming, CO2, and nitrogen deposition interactively affect a plant-pollinator mutualism. *Ecology Letters*, *15*(3), 227–234. https://doi.org/10.1111/j.1461-0248.2011.01729.x

Høye, T. T., Loboda, S., Koltz, A. M., Gillespie, M. A. K., Bowden, J. J., & Schmidt, N. M. (2021). Nonlinear trends in abundance and diversity and complex responses to climate change in Arctic arthropods. *Proceedings of the National Academy of Sciences*, *118*(2), e2002557117. https://doi.org/10.1073/pnas.2002557117

Hvitfeldt, E. (2021). *Paletteer: Comprehensive collection of color palettes*. https://github.com/EmilHvitfeldt/paletteer

Iserbyt, S., & Rasmont, P. (2013). The effect of climatic variation on abundance and diversity of bumblebees: a ten years survey in a mountain hotspot. *Annales de La Société Entomologique de France (N.S.)*, *48*(3-4), 261–273. https://doi.org/10.1080/00379271.2012.10697775

Jackson, H. M., Johnson, S. A., Morandin, L. A., Richardson, L. L., Guzman, L. M., & M'Gonigle, L. K. (2022). Climate change winners and losers among North American bumblebees. *Biology Letters*, *18*(6), 20210551. https://doi.org/10.1098/rsbl.2021.0551

Janousek, W. M., Douglas, M. R., Cannings, S., Clément, M. A., Delphia, C. M., Everett, J. G., Hatfield, R. G., Keinath, D. A., Koch, J. B. U., McCabe, L. M., Mola, J. M., Ogilvie, J. E., Rangwala, I., Richardson, L. L., Rohde, A. T., Strange, J. P., Tronstad, L. M., & Graves, T. A. (2023). Recent and future declines of a historically widespread pollinator linked to climate, land cover, and pesticides. *Proceedings of the National Academy of Sciences*, *120*(5). https://doi.org/10.1073/pnas.2211223120

Johnson, M. G., Glass, J. R., Dillon, M. E., & Harrison, J. F. (2023). How will climatic warming affect insect pollinators? *Advances in Insect Physiology*. https://doi.org/10.1016/bs.aiip.2023.01.001

Kammerer, M., Goslee, S. C., Douglas, M. R., Tooker, J. F., & Grozinger, C. M. (2021). Wild bees as winners and losers: Relative impacts of landscape composition, quality, and climate. *Global Change Biology*. https://doi.org/10.1111/gcb.15485

Kenna, D., Graystock, P., & Gill, R. J. (2023). Toxic temperatures: Bee behaviours exhibit divergent pesticide toxicity relationships with warming. *Global Change Biology*. https://doi.org/10.1111/gcb.16671

Kenna, D., Pawar, S., & Gill, R. J. (2021). Thermal flight performance reveals impact of warming on bumblebee foraging potential. *Functional Ecology*. https://doi.org/10.1111/1365-2435.13887

763 Kerr, J. T., Pindar, A., Galpern, P., Packer, L., Potts, S. G., Roberts, S. M., Rasmont, P.,
764 Schweiger, O., Colla, S. R., Richardson, L. L., Wagner, D. L., Gall, L. F., Sikes, D. S., & Pantoja, A.
765 (2015). Climate change impacts on bumblebees converge across continents. *Science*,
766 *349*(6244), 177–180. https://doi.org/10.1126/science.aaa7031

767 Kim, H., McComb, B. C., Frey, S. J. K., Bell, D. M., & Betts, M. G. (2022). Forest microclimate
768 and composition mediate long-term trends of breeding bird populations. *Global Change*
769 *Biology*, *28*(21), 6180–6193. https://doi.org/10.1111/gcb.16353

770 Lehmann, P., Ammunét, T., Barton, M., Battisti, A., Eigenbrode, S. D., Jepsen, J. U., Kalinkat, G.,
771 Neuvonen, S., Niemelä, P., Terblanche, J. S., Økland, B., & Björkman, C. (2020). Complex
772 responses of global insect pests to climate warming. *Frontiers in Ecology and the*
773 *Environment*, *18*(3), 141–150. https://doi.org/10.1002/fee.2160

774 Looney, C., Strange, J. P., Freeman, M., & Jennings, D. (2019). The expanding Pacific
775 Northwest range of Bombus impatiens Cresson and its establishment in Washington State.
776 *Biological Invasions*, *21*(6), 1879–1885. https://doi.org/10.1007/s10530-019-01970-6

777 Lopez, H., West, R., Dong, S., Goni, G., Kirtman, B., Lee, S.-K., & Atlas, R. (2018). Early
778 emergence of anthropogenically forced heat waves in the western United States and Great
779 Lakes. *Nature Climate Change*, *8*(5), 414–420. https://doi.org/10.1038/s41558-018-0116-
780 y

781 Lüdecke, D., Ben-Shachar, M. S., Patil, I., Waggoner, P., & Makowski, D. (2021). performance:
782 An R package for assessment, comparison and testing of statistical models. *Journal of Open*
783 *Source Software*, *6*(60), 3139. https://doi.org/10.21105/joss.03139

784 Maebe, K., Hart, A. F., Marshall, L., Vandamme, P., Vereecken, N. J., Michez, D., & Smagghe, G.
785 (2021). Bumblebee resilience to climate change, through plastic and adaptive responses.
786 *Global Change Biology*, *27*(18), 4223–4237. https://doi.org/10.1111/gcb.15751

787 Maron, M., McAlpine, C. A., Watson, J. E. M., Maxwell, S., & Barnard, P. (2015). Climate-
788 induced resource bottlenecks exacerbate species vulnerability: a review. *Diversity and*
789 *Distributions*, *21*(7), 731–743. https://doi.org/10.1111/ddi.12339

790 Meehl, G. A., & Tebaldi, C. (2004). More Intense, More Frequent, and Longer Lasting Heat
791 Waves in the 21st Century. *Science*, *305*(5686), 994–997.
792 https://doi.org/10.1126/science.1098704

793 Microsoft, & Weston, S. (2022). *Foreach: Provides foreach looping construct*.
794 https://CRAN.R-project.org/package=foreach

795 Neff, F., Korner-Nievergelt, F., Rey, E., Albrecht, M., Bollmann, K., Cahenzli, F., Chittaro, Y.,
796 Gossner, M. M., Martínez-Núñez, C., Meier, E. S., Monnerat, C., Moretti, M., Roth, T., Herzog,
797 F., & Knop, E. (2022). Different roles of concurring climate and regional land-use changes in
798 past 40 years' insect trends. *Nature Communications*, *13*(1), 7611.
799 https://doi.org/10.1038/s41467-022-35223-3

800 Ockendon, N., Baker, D. J., Carr, J. A., White, E. C., Almond, R. E. A., Amano, T., Bertram, E.,
801 Bradbury, R. B., Bradley, C., Butchart, S. H. M., Doswald, N., Foden, W., Gill, D. J. C., Green, R.
802 E., Sutherland, W. J., Tanner, E. V. J., & Pearce-Higgins, J. W. (2014). Mechanisms
803 underpinning climatic impacts on natural populations: altered species interactions are

804 more important than direct effects. *Global Change Biology*, *20*(7), 2221–2229.
805 https://doi.org/10.1111/gcb.12559

806 Ogilvie, J. E., Griffin, S. R., Gezon, Z. J., Inouye, B. D., Underwood, N., Inouye, D. W., & Irwin, R.
807 E. (2017). Interannual bumble bee abundance is driven by indirect climate effects on floral
808 resource phenology. *Ecology Letters*, *20*(12), 1507–1515.
809 https://doi.org/10.1111/ele.12854

810 Oliver, I., Dorrough, J., Doherty, H., & Andrew, N. R. (2016). Additive and synergistic effects
811 of land cover, land use and climate on insect biodiversity. *Landscape Ecology*, *31*(10), 2415–
812 2431. https://doi.org/10.1007/s10980-016-0411-9

813 Oliver, T. H., Marshall, H. H., Morecroft, M. D., Brereton, T., Prudhomme, C., & Huntingford, C.
814 (2015). Interacting effects of climate change and habitat fragmentation on drought-
815 sensitive butterflies. *Nature Climate Change*, *5*(10), 941–945.
816 https://doi.org/10.1038/nclimate2746

817 Outhwaite, C. L., McCann, P., & Newbold, T. (2022). Agriculture and climate change are
818 reshaping insect biodiversity worldwide. *Nature*, 1–6. https://doi.org/10.1038/s41586-
819 022-04644-x

820 Oyen, K. J., Giri, S. & Dillon, M. E. (2016). Altitudinal variation in bumble bee (Bombus)
821 critical thermal limits. *J Therm Biol* 59, 52–57.
822 https://doi.org/10.1016/j.jtherbio.2016.04.015

823 Palmier, K., Sheffield, C., & Sheffield, C. (2019). First records of the Common Eastern
824 Bumble Bee, Bombus impatiens Cresson (Hymenoptera: Apidae, Apinae, Bombini) from the
825 Prairies Ecozone in Canada. *Biodiversity Data Journal*, *7*(7), e30953.
826 https://doi.org/10.3897/bdj.7.e30953

827 PARMESAN, C. (2007). Influences of species, latitudes and methodologies on estimates of
828 phenological response to global warming. *Global Change Biology*, *13*(9), 1860–1872.
829 https://doi.org/10.1111/j.1365-2486.2007.01404.x

830 Pebesma, E. (2018). Simple Features for R: Standardized Support for Spatial Vector Data.
831 *The R Journal*, *10*(1), 439–446. https://doi.org/10.32614/RJ-2018-009

832 Pedersen, E. J., Miller, D. L., Simpson, G. L., & Ross, N. (2019). Hierarchical generalized
833 additive models in ecology: an introduction with mgcv. *PeerJ*, *7*, e6876.
834 https://doi.org/10.7717/peerj.6876

835 Pincebourde, S., & Woods, H. A. (2020). There is plenty of room at the bottom:
836 microclimates drive insect vulnerability to climate change. *Current Opinion in Insect*
837 *Science*, *41*, 63–70. https://doi.org/10.1016/j.cois.2020.07.001

838 Princé, K., & Zuckerberg, B. (2015). Climate change in our backyards: the reshuffling of
839 North America's winter bird communities. *Global Change Biology*, *21*(2), 572–585.
840 https://doi.org/10.1111/gcb.12740

841 Pyke, G. H., Thomson, J. D., Inouye, D. W., & Miller, T. J. (2016). Effects of climate change on
842 phenologies and distributions of bumble bees and the plants they visit. *Ecosphere*, *7*(3).
843 https://doi.org/10.1002/ecs2.1267

R Core Team. (2017). *R: A language and environment for statistical computing*. R Foundation for Statistical Computing. https://www.R-project.org/

Raven, P. H., & Wagner, D. L. (2021). Agricultural intensification and climate change are rapidly decreasing insect biodiversity. *Proceedings of the National Academy of Sciences*, *118*(2), e2002548117. https://doi.org/10.1073/pnas.2002548117

Richardson, L. et al., (2023). Bumble Bees of North America (https://www.leifrichardson.org/bbna.html)

Settele, J., Bishop, J., & Potts, S. G. (2016). Climate change impacts on pollination. *Nature Plants*, *2*(7), 16092. https://doi.org/10.1038/nplants.2016.92

Simpson, G. L. (2018). Modelling Palaeoecological Time Series Using Generalised Additive Models. *Frontiers in Ecology and Evolution*, *6*, 149. https://doi.org/10.3389/fevo.2018.00149

Simpson, G. L. (2023). *gratia: Graceful ggplot-based graphics and other functions for GAMs fitted using mgcv*. https://gavinsimpson.github.io/gratia/

Sirois-Delisle, C., & Kerr, J. T. (2018). Climate change-driven range losses among bumblebee species are poised to accelerate. *Scientific Reports*, *8*(1), 14464. https://doi.org/10.1038/s41598-018-32665-y

Soroye, P., Newbold, T., & Kerr, J. (2020). Climate change contributes to widespread declines among bumble bees across continents. *Science*, *367*(6478), 685–688. https://doi.org/10.1126/science.aax8591

Szabo, N. D., Colla, S. R., Wagner, D. L., Gall, L. F., & Kerr, J. T. (2012). Do pathogen spillover, pesticide use, or habitat loss explain recent North American bumblebee declines?: Causes of bumblebee declines. *Conservation Letters*, *5*(3), 232–239. https://doi.org/10.1111/j.1755-263x.2012.00234.x

Thompson, V., Kennedy-Asser, A. T., Vosper, E., Lo, Y. T. E., Huntingford, C., Andrews, O., Collins, M., Hegerl, G. C., & Mitchell, D. (2022). The 2021 western North America heat wave among the most extreme events ever recorded globally. *Science Advances*, *8*(18), eabm6860. https://doi.org/10.1126/sciadv.abm6860

Tingley, M. W., & Beissinger, S. R. (2013). Cryptic loss of montane avian richness and high community turnover over 100 years. *Ecology*, *94*(3), 598–609. https://doi.org/10.1890/12-0928.1

Warren, M. S., Hill, J. K., Thomas, J. A., Asher, J., Fox, R., Huntley, B., Roy, D. B., Telfer, M. G., Jeffcoate, S., Harding, P., Jeffcoate, G., Willis, S. G., Greatorex-Davies, J. N., Moss, D., & Thomas, C. D. (2001). Rapid responses of British butterflies to opposing forces of climate and habitat change. *Nature*, *414*(6859), 65–69. https://doi.org/10.1038/35102054

Whitehorn, P. R., Seo, B., Comont, R. F., Rounsevell, M., & Brown, C. (2022). The effects of climate and land use on British bumblebees: Findings from a decade of citizen-science observations. *Journal of Applied Ecology*, *59*(7), 1837–1851. https://doi.org/10.1111/1365-2664.14191

883 Wickham, H., Averick, M., Bryan, J., Chang, W., McGowan, L. D., François, R., Grolemund, G.,
884 Hayes, A., Henry, L., Hester, J., Kuhn, M., Pedersen, T. L., Miller, E., Bache, S. M., Müller, K.,
885 Ooms, J., Robinson, D., Seidel, D. P., Spinu, V., … Yutani, H. (2019). Welcome to the tidyverse.
886 *Journal of Open Source Software*, *4*(43), 1686. https://doi.org/10.21105/joss.01686

887 Wood, S. N. (2011). Fast stable restricted maximum likelihood and marginal likelihood
888 estimation of semiparametric generalized linear models. *Journal of the Royal Statistical*
889 *Society (B)*, *73*(1), 3–36.